

# New Beam Test Results of 3D Pixel Detectors Constructed With poly-crystalline CVD diamonds

---

## The RD42 Collaboration

M. Reichmann<sup>\*24</sup>, A. Alexopoulos<sup>3</sup>, M. Artuso<sup>20</sup>, F. Bachmair<sup>24</sup>, L. Băni<sup>24</sup>,  
M. Bartosik<sup>3</sup>, H. Beck<sup>23</sup>, V. Bellini<sup>2</sup>, V. Belyaev<sup>12</sup>, B. Bentele<sup>19</sup>, A. Bes<sup>27</sup>, J-M. Brom<sup>7</sup>,  
M. Bruzzi<sup>4</sup>, G. Chiodini<sup>26</sup>, D. Chren<sup>18</sup>, V. Cindro<sup>9</sup>, G. Claus<sup>7</sup>, J. Collot<sup>27</sup>, J. Cumalat<sup>19</sup>,  
A. Dabrowski<sup>3</sup>, R. D'Alessandro<sup>4</sup>, D. Dauvergne<sup>27</sup>, W. de Boer<sup>10</sup>, C. Dorfer<sup>24</sup>,  
M. Dünser<sup>3</sup>, G. Eigen<sup>30</sup>, V. Eremin<sup>6</sup>, G. Forcolin<sup>22</sup>, J. Forneris<sup>15</sup>, L. Gallin-Martel<sup>27</sup>,  
M-L. Gallin-Martel<sup>27</sup>, K. K. Gan<sup>13</sup>, M. Gastal<sup>3</sup>, M. Goffe<sup>7</sup>, J. Goldstein<sup>17</sup>, A. Golubev<sup>8</sup>,  
A. Gorišek<sup>9</sup>, E. Grigoriev<sup>8</sup>, J. Grosse-Knetter<sup>23</sup>, A. Grummer<sup>21</sup>, M. Guthoff<sup>3</sup>, B. Hiti<sup>9</sup>,  
D. Hits<sup>24</sup>, M. Hoeferkamp<sup>21</sup>, T. Hofmann<sup>3</sup>, J. Hosselet<sup>7</sup>, F. Hügging<sup>1</sup>, C. Hutton<sup>17</sup>,  
J. Janssen<sup>1</sup>, H. Kagan<sup>13</sup>, K. Kanxheri<sup>28</sup>, R. Kass<sup>13</sup>, M. Kis<sup>5</sup>, G. Kramberger<sup>9</sup>,  
S. Kuleshov<sup>8</sup>, A. Lacoste<sup>27</sup>, S. Lagomarsino<sup>4</sup>, A. Lo Giudice<sup>15</sup>, I. Lopez Paz<sup>22</sup>,  
E. Lukosi<sup>25</sup>, C. Maazouzi<sup>7</sup>, I. Mandić<sup>9</sup>, C. Mathieu<sup>7</sup>, M. Menichelli<sup>28</sup>, M. Mikuž<sup>9</sup>,  
A. Morozzi<sup>28</sup>, J. Moss<sup>29</sup>, R. Mountain<sup>20</sup>, A. Oh<sup>22</sup>, P. Olivero<sup>15</sup>, D. Passeri<sup>28</sup>,  
H. Pernegger<sup>3</sup>, R. Perrino<sup>26</sup>, F. Picollo<sup>15</sup>, M. Pomorski<sup>11</sup>, R. Potenza<sup>2</sup>, A. Quadt<sup>23</sup>,  
F. Rarbi<sup>27</sup>, A. Re<sup>15</sup>, S. Roe<sup>3</sup>, D. A. Sanz Becerra<sup>24</sup>, M. Scaringella<sup>4</sup>, C. J. Schmidt<sup>5</sup>,  
S. Schnetzer<sup>14</sup>, E. Schioppa<sup>3</sup>, S. Sciortino<sup>4</sup>, A. Scorzoni<sup>28</sup>, S. Seidel<sup>21</sup>, L. Servoli<sup>28</sup>,  
D. S. Smith<sup>13</sup>, B. Sopko<sup>18</sup>, V. Sopko<sup>18</sup>, S. Spagnolo<sup>26</sup>, S. Spanier<sup>25</sup>, K. Stenson<sup>19</sup>,  
R. Stone<sup>14</sup>, B. Stugu<sup>30</sup>, C. Sutura<sup>2</sup>, M. Traeger<sup>5</sup>, W. Trischuk<sup>16</sup>, M. Truccato<sup>15</sup>,  
C. Tuve<sup>2</sup>, J. Velthuis<sup>17</sup>, N. Venturi<sup>3</sup>, S. Wagner<sup>19</sup>, R. Wallny<sup>24</sup>, J. C. Wang<sup>20</sup>,  
N. Wermes<sup>1</sup>, M. Yamouni<sup>27</sup>, J. Zalieckas<sup>30</sup> and M. Zavrtanik<sup>9</sup>

<sup>1</sup>Universität Bonn, Bonn, Germany

<sup>2</sup>INFN/University of Catania, Catania, Italy

<sup>3</sup>CERN, Geneva, Switzerland

<sup>4</sup>INFN/University of Florence, Florence, Italy

<sup>5</sup>GSI, Darmstadt, Germany

<sup>6</sup>Ioffe Institute, St. Petersburg, Russia

<sup>7</sup>IPHC, Strasbourg, France

<sup>8</sup>ITEP, Moscow, Russia

<sup>9</sup>Jožef Stefan Institute, Ljubljana, Slovenia

<sup>10</sup>Universität Karlsruhe, Karlsruhe, Germany

<sup>11</sup>CEA-LIST Technologies Avancees, Saclay, France

<sup>12</sup>MEPHI Institute, Moscow, Russia

<sup>13</sup>The Ohio State University, Columbus, OH, USA

<sup>14</sup>Rutgers University, Piscataway, NJ, USA

<sup>15</sup>University of Torino, Torino, Italy

<sup>16</sup>University of Toronto, Toronto, ON, Canada

<sup>17</sup>University of Bristol, Bristol, UK

<sup>18</sup>*Czech Technical University, Prague, Czech Republic*

<sup>19</sup>*University of Colorado, Boulder, CO, USA*

<sup>20</sup>*Syracuse University, Syracuse, NY, USA*

<sup>21</sup>*University of New Mexico, Albuquerque, NM, USA*

<sup>22</sup>*University of Manchester, Manchester, UK*

<sup>23</sup>*Universität Göttingen, Göttingen, Germany*

<sup>24</sup>*ETH Zürich, Zürich, Switzerland*

<sup>25</sup>*University of Tennessee, Knoxville, TN, USA*

<sup>26</sup>*INFN-Lecce, Lecce, Italy*

<sup>27</sup>*LPSC-Grenoble, Grenoble, France*

<sup>28</sup>*INFN-Perugia, Perugia, Italy*

<sup>29</sup>*California State University, Sacramento, CA, USA*

<sup>30</sup>*University of Bergen, Bergen, Norway*

*E-mail: michael.reichmann@cern.ch*

As nuclear and high energy facilities around the world strive for higher and higher energies and intensities, more radiation tolerant technologies are required to withstand the increasing radiation doses. As a possible candidate we present a novel detector design - namely 3D Detectors - based on poly-crystalline CVD diamond sensors with a pixel readout. The fabrication of these 3D detectors as well the results of the most recent detectors are shown. We measured the efficiency and signal response of two 3D diamond detectors with  $50 \times 50 \mu\text{m}$  cell sizes using pixel readout chip technologies currently used at CMS and ATLAS. The maximum measured efficiency was 99.2 %.

*29th International Symposium on Lepton Photon Interactions at High Energies  
5-10 August 2019  
Westin Harbour Castle, Toronto Canada*

---

\*Speaker.

## 1. Introduction

The radiation levels of the High-Luminosity-LHC (HL-LHC) are expected to be a big challenge for the future detectors. By 2028 experiments must be prepared for an instantaneous luminosity of  $7.5 \cdot 10^{34} \text{ cm}^{-2} \text{ s}^{-1}$ . In this environment the innermost tracking layer at a transverse distance of  $\sim 30 \text{ mm}$  to the interaction point will be exposed to a total fluence of  $2 \cdot 10^{16} \text{ n}_{\text{eq}}/\text{cm}^2$  [1]. The expected lifetime of the current planar silicon tracking detectors would be about one year in such an environment.

Chemical Vapour Deposition (CVD) diamond is investigated by the RD42 collaboration as a possible detector material [2]. Its minimum lattice displacement energy of  $43 \text{ eV/atom}$  [3] makes it intrinsically radiation tolerant and the band gap of  $5.5 \text{ eV}$  greatly simplifies the construction of the detectors as well as guarantees negligible leakage currents. Compared to analogous silicon detectors, it was shown that diamond is at a minimum three times more radiation tolerant [4], collects the charges at least two times faster [5] and conducts heat four times more efficiently [6].

After the doses expected in the HL-LHC, all detector materials become trap limited with a *schubweg*, the average drift distance before a free charge carrier gets trapped, below  $75 \mu\text{m}$  [7, 8]. Therefore RD42 collaboration is studying a novel detector design in diamond, namely 3D detectors. This detector design places column-like electrodes inside the detector material. Therefore the drift distance an electron-hole pair must undergo to reach an electrode can be reduced below the *schubweg* of an irradiated sensor without reducing the amount of created electron-hole pairs. Details about the working principle can be found in [9].

## 2. 3D Pixel Detectors

### 2.1 Fabrication

All devices discussed in this article were constructed with poly-crystalline Chemical Vapour Deposition (pCVD) diamond. The sensors are thin plates with a thickness of  $\sim 500 \mu\text{m}$  and a side length of  $\sim 5 \text{ mm}$ . In order to manufacture the electrodes in diamond, columns were fabricated perpendicular to the large side using a  $130 \text{ fs}$  laser with a wavelength of  $800 \text{ nm}$  which converts the diamond into a electrically resistive mixture of different carbon phases [10]. A Spatial Light Modulator (SLM) [11] was used to correct spherical aberrations during fabrication. This helped to achieve the high column yield of  $\gtrsim 99.8 \%$ , a column diameter of  $2.6 \mu\text{m}$  and a resistivity of the columns of the order of  $0.1 \sim 1 \Omega \text{ cm}$ . The yield was measured by manually counting missing or broken columns and the diameter was optically measured. The columns are not drilled completely through the diamond, but with a gap of  $15 \mu\text{m}$  to the opposite surface to avoid high voltage breakdown at the operated electric fields of up to  $2 \text{ V}/\mu\text{m}$ . The detector was constructed by ganging all bias columns together with a metallisation on one surface and metallise the single readout columns on the other surface in order to bump bond the sensor to the readout electronics.

The detectors described herein were connected to two different readout chips (ROCs), which is why different bonding processes, as shown in Figures 1, had to be used. For both of these detectors a 3D cell size of  $50 \mu\text{m} \times 50 \mu\text{m}$  was chosen. Since the layout of the ROCs had a different pixel pitch several cells were ganged together by connecting several readout columns with the surface metallisation. The detector B6 was connected to the PSI46digV2.1respin ROC [12] with a  $3 \times 2$

cell ganging to match the pixel pitch of  $150\text{ }\mu\text{m} \times 100\text{ }\mu\text{m}$ . It was bump bonded to the ROC at the Nanofabrication Lab at the Princeton University with indium. This was achieved by putting equal height indium columns on both ROC and the sensor and then pressing them together without reflow 1a. The detector B5 was connected to the FE-I4B ROC [13] with a  $5 \times 1$  cell ganging due to the pixel pitch of  $250\text{ }\mu\text{m} \times 50\text{ }\mu\text{m}$ . The bump bonding for this sensor was performed at IFAE-CNM in Barcelona by an adapted process with tin-silver bumps 1b.

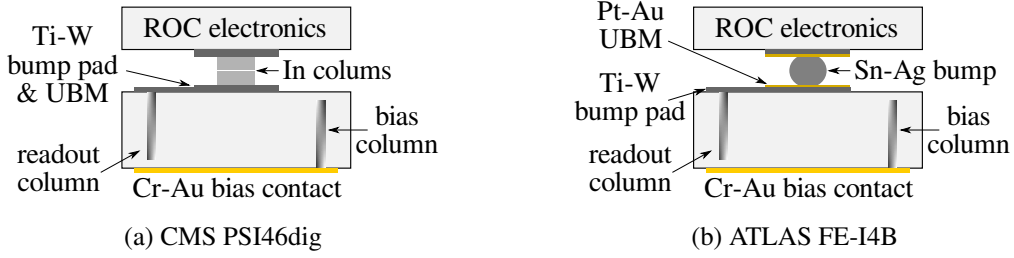


Figure 1: Bump Bonding and metallisation for two different ROCs.

Both devices have  $\sim 4000$  3D cells, where one cell consists of four bias electrodes and one readout electrode in the centre. Since the bias electrodes are shared between the cells,  $\sim 7000$  columns had to be drilled to build such a device. The details of the two devices are listed in Table 1. Except for the different readout the sensors are very similar. Photographs of the assembled 3D detectors on the ROCs are shown in Figure 2.

	1	2
readout chip (ROC)	PSI46digv2.1respin	FE-I4B
pixel pitch	$150\text{ }\mu\text{m} \times 100\text{ }\mu\text{m}$	$250\text{ }\mu\text{m} \times 50\text{ }\mu\text{m}$
3D cell size	$50\text{ }\mu\text{m} \times 50\text{ }\mu\text{m}$	$50\text{ }\mu\text{m} \times 50\text{ }\mu\text{m}$
ganging	$3 \times 2$	$5 \times 1$
size	$4.85\text{ mm} \times 4.90\text{ mm}$	$4.90\text{ mm} \times 4.94\text{ mm}$
thickness	$500\text{ }\mu\text{m}$	$510\text{ }\mu\text{m}$
$50\text{ pixels} \times 50\text{ pixels}$	$67 \times 53$	$53 \times 67$
3D columns	7223	7223
column diameter	$2.6\text{ }\mu\text{m}$	$2.6\text{ }\mu\text{m}$
active area	$3.45\text{ mm} \times 3.19\text{ mm}$	$3.2\text{ mm} \times 3.5\text{ mm}$
bump bonding	tin silver (IFAE)	indium (Princeton)

Table 1: Properties of the 3D diamond detectors.

## 2.2 Results of Detector 1 ( $3 \times 2$ )

This detector was tested with pixel telescopes in beam lines at Paul Scherrer Institut (PSI) and the SPS facility at CERN in order to get both measurements at high rates as well as with high tracking resolution. The preliminary beam test results show that, relative to a planar silicon device, the efficiency within a selected fiducial area was 99.2 %. Where the hit efficiency was defined as the percentage of hits in the 3D pixel detector when a particle track traversed the detector. This value was measured at both beam test facilities.

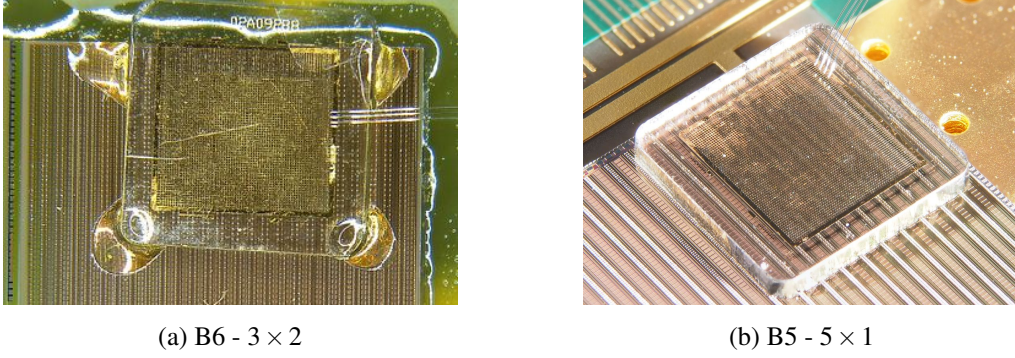


Figure 2: Assembled 3D pixel detectors.

The fiducial area was selected such as to exclude non-working 3D cells found by visual inspection, which can happen due to broken or missing columns or due to metallisation issues, where the metal is not properly connected to the electrodes. A small discrepancy between a 3D and a fully efficient planar device is partly expected due to the relative inefficiency of the columns themselves. The area of the 3D columns compared to the whole cell is 0.4 %.

Figure 3 shows that the efficiency of the detector plateaus at a voltage of 30 V. This demonstrates that the device already operates well at very low voltages compared to a planar diamond detector. The efficiency at both facilities agrees well, which shows that the detector is independent of the different particle energies and intensities which were used.

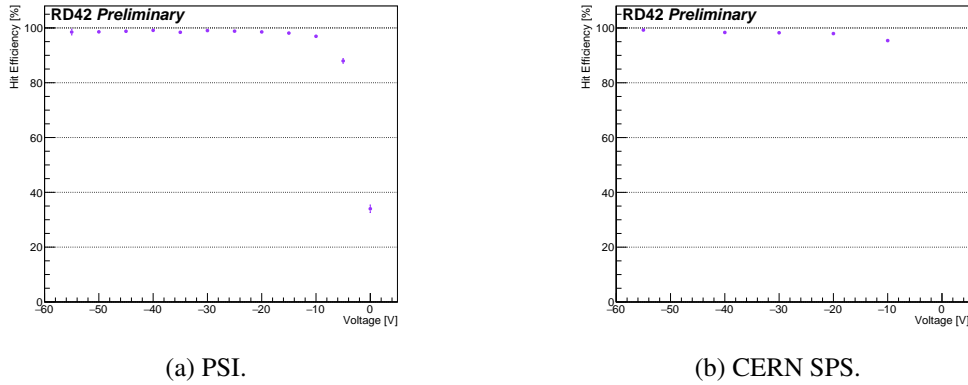


Figure 3: Hit efficiency vs. bias voltage.

The preliminary analysis of the pulse height distribution for the measurements at CERN yields a mean value of  $\sim 14$  ke. The precise pulse height calibration of the ROC is currently being studied.

### 2.3 Results of Detector 2 (5x1)

This device was solely tested at the CERN SPS beam line with 120 GeV hadrons. The tracking reconstruction was done with a using resolution beam telescope, with a spatial resolution of  $3 \mu\text{m}$  at the device under test so that the efficiency could be mapped to the spatial coordinates.

The first results are shown in Figure 4. The analysis yields an efficiency of 98.2 % in the contiguous fiducial area (Figure 4a). As shown in Figure 4b, the detector reaches the same efficiency for all tested voltages. The efficiency being lower than 99 % is most likely due to issues with the bump bonding or the metallisation as suggested by the pattern of inefficient patches in the efficiency map. The preliminary pulse

height in the fiducial region was  $\sim 14$  ke which is consistent with the result of the first detector. The precise pulse height calibration for the FE-I4B ROC is in the process of being performed.

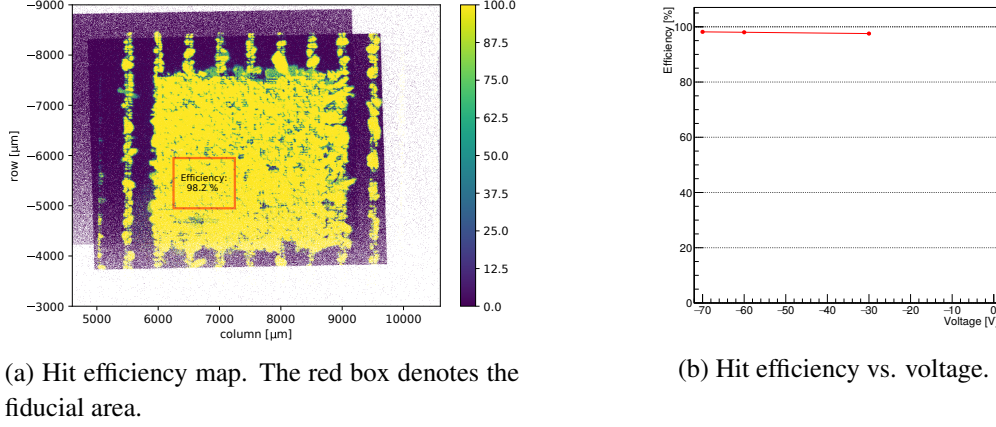


Figure 4: Results of the FE-I4 readout.

### 3. Conclusion

We demonstrated a progress in the development of radiation tolerant particle detectors based on pCVD diamonds. We showed to working prototypes of 3D diamond pixel detectors with sizes of  $50\,\mu\text{m} \times 50\,\mu\text{m}$  and column diameters of  $2.6\,\mu\text{m}$ . The shown devices had a total number of 3551 cells and the efficiency of the column drilling process is above 99.8 %. The first prototypes of small cell 3D diamond pixel detectors read out more charge than any planar pCVD diamond detector. The measured relative hit efficiency of the 3D pixel detectors reached a maximum of 99.2 % compared to a planar silicon device.

### Acknowledgements

We want to thank Bert Harrop at the Physics Department of the Princeton University as well as Mokhtar Chmeissani, Sebastian Grinstein and David Vazquez Furelos at IFAE for bump bonding the devices. Also our thanks goes to Patrick Salter from the University of Oxford for drilling the 3D column in the diamond sensors. The research leading to these results received funding from the European Union’s Horizon 2020 research and innovation program under grant agreement No. 654168. This work was also partially supported by the Swiss National Science Foundation grant #20FL20\_154216, ETH grant 51 15-1, the Swiss Government Excellence Scholarship ESKAS No. 2015.0808, the Royal Society Grant UF120106, the UK Science and Technology Facilities Council Grant ST/P002846/1 and the U.S. Department of Energy through grant DE-SC0010061

### References

- [1] D. Contardo, M. Klute, J. Mans, L. Silvestris, and J. Butler, “Technical Proposal for the Phase-II Upgrade of the CMS Detector,” Tech. Rep. CERN-LHCC-2015-010. LHCC-P-008. CMS-TDR-15-02, Geneva, Jun 2015.
- [2] H. Kagan *et al.*, “Development of Diamond Tracking Detectors for High Luminosity Experiments at the LHC, HL-LHC and Beyond,” Tech. Rep. CERN-LHCC-2018-015. LHCC-SR-005, CERN, Geneva, May 2018.

- [3] J. Koike, D. M. Parkin, and T. E. Mitchell, “Displacement threshold energy for type iia diamond,” *Applied Physics Letters*, vol. 60, no. 12, pp. 1450–1452, 1992.
- [4] W. de Boer *et al.*, “Radiation hardness of diamond and silicon sensors compared,” *Physica Status Solidi Applied Research*, vol. 204, pp. 3004–3010, Sep 2007.
- [5] H. Pernegger *et al.*, “Charge-carrier properties in synthetic single-crystal diamond measured with the transient-current technique,” *J. Appl. Phys.*, vol. 97, no. 7, pp. 73704–1–9, 2005.
- [6] S. Zhao, *Characterization of the electrical properties of polycrystalline diamond films*. PhD thesis, The Ohio State University, 1994.
- [7] H. Feick, “Radiation tolerance of silicon particle detectors for high-energy physics experiments,” 1997. Presented on Aug 1997.
- [8] J.-W. Tsung, M. Havranek, F. Hugging, H. Kagan, H. Kruger, and N. Wermes, “Signal and noise of Diamond Pixel Detectors at High Radiation Fluences. Signal and noise of Diamond Pixel Detectors at High Radiation Fluences,” *JINST*, vol. 7, p. P09009, Jun 2012.
- [9] S. Parker, C. Kenney, and J. Segal, “3D - A proposed new architecture for solid-state radiation detectors,” *Nuclear Instruments and Methods in Physics Research Section A: Accelerators, Spectrometers, Detectors and Associated Equipment*, vol. 395, no. 3, pp. 328 – 343, 1997.
- [10] S. M. Pimenov *et al.*, “Femtosecond laser microstructuring in the bulk of diamond,” *Diamond and Related Materials*, vol. 18, no. 2, pp. 196 – 199, 2009.
- [11] B. Sun, P. S. Salter, and M. J. Booth, “High conductivity micro-wires in diamond following arbitrary paths,” *Applied Physics Letters*, vol. 105, no. 23, p. 231105, 2014.
- [12] A. Kornmayer, T. Müller, and U. Husemann, “Studies on the response behaviour of pixel detector prototypes at high collision rates for the CMS experiment,” Nov 2015. Presented 04 Dec 2015.
- [13] M. Garcia-Sciveres *et al.*, “The FE-I4 Pixel Readout Integrated Circuit,” Tech. Rep. ATL-UPGRADE-PROC-2010-001, CERN, Geneva, Jan 2010.